Journal of Alloys and Compounds 509 (2011) 10062–10065

Contents lists available at ScienceDirect

Journal of Alloys and Compounds

journal homepage: www.elsevier.com/locate/jallcom

Effect of annealing temperature on optical band-gap of amorphous indium zinc oxide film

Ju-Won Jeon[a], Dae-Woo Jeon[a], Trilochan Sahoo[a], Myoung Kim[a], Jong-Hyeob Baek[b], Jessica Lynn Hoffman[c], Nam Soo Kim[c], In-Hwan Lee[a,*]

[a] School of Advanced Materials Engineering and Research Center for Advanced Materials Development, Chonbuk National University, Jeonju, Chonbuk 561-756, Republic of Korea
[b] LED Device Team, Korea Photonics Technology Institute, Gwangju 500-779, Republic of Korea
[c] Department of Metallurgical and Materials Engineering, The University of Texas at El Paso, El Paso, TX 79968, USA

ARTICLE INFO

Article history:
Received 27 June 2011
Accepted 6 August 2011
Available online 12 August 2011

Keywords:
InZnO
Annealing temperature
Optical band gap
Burstein-Moss effect

ABSTRACT

The effect of annealing temperature on the electrical and optical properties of indium zinc oxide (IZO) (In_2O_3:ZnO = 90:10 wt.%) thin films has been investigated. The IZO thin films were deposited on glass substrates by radio frequency magnetron sputtering and then subjected to annealing in a mixed ambient of air and oxygen at 100, 200 and 300 °C. All the IZO films were found to have amorphous structure. With the increase of the annealing temperature, the carrier concentration decreased and the resistivity increased. The average transmittance of IZO thin films decreased slightly with annealing temperature. Interestingly, a systematic reduction of the optical band-gap from 3.79 eV to 3.67 eV was observed with annealing temperature. The change in optical band-gap was observed to be caused predominantly by Burstein-Moss band-gap widening effect suggesting unusual absence of band narrowing effect. The effects on optical and electrical properties of IZO films have been discussed in detail.

1. Introduction

Indium zinc oxide (IZO) is one of the important transparent conducting oxide (TCO) materials and is widely used as transparent electrode in various kinds of devices such as solar cells, thin film transistors and organic light emitting diodes. The electrical conductivity, transparency, thermal stability, durability, etchability and resistance to hydrogen plasma make this material suitable for a wide range of device applications [1–5]. IZO is preferred because of its superior work function, higher transmittance and higher etching rate [6]. Additionally, amorphous IZO films prepared by the sputtering method under the similar conditions could have a smoother surface morphology and smaller stress concentration than other TCO films [7]. The properties of IZO and other TCOs are largely related to their band-gaps. For the application of IZO in optoelectronic devices, one of the most relevant properties is the optical band-gap. The optical band gap closely depends on the change of carrier concentration, which might have caused by growth conditions as annealing treatment, and doping. In degenerated semiconductors the relation between the optical band-gap and the carrier concentration is explained by the Burstein-Moss (BM) effect and band-gap narrowing effect [8,9]. The band-gap narrowing results from band-gap renormalization due to many-body interaction in the conduction band and valence band. The BM effect leads to optical band-gap widening by the blocking of lower (higher) states in the conduction (valence) band of n-type (p-type) semiconductors. In degenerate semiconductors with high carrier concentration band gap narrowing effect is generally expected. Apparent absence of narrowing effect or domination of the BM effect is not common.

In this study, we report the anomalous observation of domination of the BM effect on the optical band gap of IZO thin films. The effects of annealing temperature on the optical and electrical properties of IZO thin films deposited by radio frequency magnetron sputtering were studied. The optical band-gap was shifted systematically due to the change of the carrier concentration with the annealing temperature. The shift of band gap is discussed in detail and could be explained without resorting to band gap narrowing effects.

2. Experimental

The IZO films were deposited on glass substrates (Corning EAGLE 2000) at room temperature by radio frequency magnetron sputtering using a mixed oxide target of In_2O_3 and ZnO with a weight ratio of 9:1 (4 in., 99.99% pure). The films were deposited under argon ambient with the substrate-to-target distance of 10 cm. During the deposition the radio frequency power and the gas pressure were maintained at 260 W and 10 m Torr, respectively. The thickness of the as-deposited IZO films was found to be ~200 nm. The as-deposited films were annealed at different temperatures in a ceramic tube furnace for 1 h in a mixed atmosphere of air and oxygen. The

* Corresponding author. Tel.: +82 63 270 2292; fax: +82 63 270 2305.
E-mail address: ihlee@jbnu.ac.kr (I.-H. Lee).

0925-8388/$ – see front matter
doi:10.1016/j.jallcom.2011.08.033

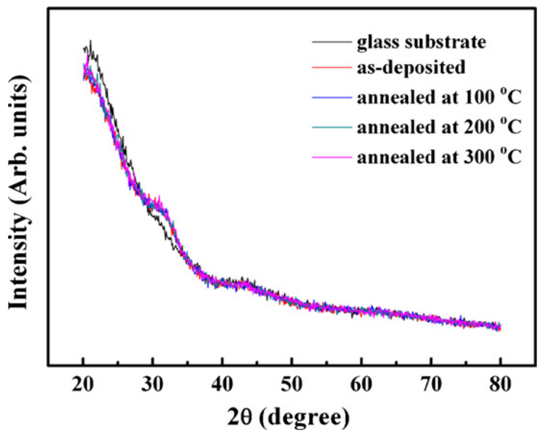

Fig. 1. XRD patterns of the as-grown IZO film and the films annealed at RT, 100, 200 and 300 °C.

crystal structure of the films was characterized by X-ray diffraction (XRD, Philips X'pert X-ray diffractometer). The electrical resistivity, carrier concentration and Hall mobility were determined by Hall effect measurements (Biorad HL5500) using the Van der Pauw geometry at a constant magnetic field of 0.5 T. The optical transmittance was measured in the wavelength range of 300–800 nm using a UV–vis–NIR double beam spectrophotometer (UV-3100 PC, Shimadzu).

3. Results and discussion

Fig. 1 shows the XRD pattern of the as-deposited and the IZO films annealed at 100–300 °C. All the films were amorphous, as indicated by the broad low-intensity hump at $2\theta = 33°$ [4]. The XRD results are in agreement with the studies by Ito et al. regarding the crystallization temperature of amorphous IZO [11]. It was reported that amorphous IZO exhibited higher thermal stability up to 400–500 °C compared to amorphous ITO having a crystallization temperature of 170–180 °C [11,12].

The electrical properties of IZO thin films were found to vary depending on the annealing conditions. The measured changes in electrical resistivity, carrier concentration, and Hall mobility with annealing temperature are presented in Fig. 2. One can observe that the above parameters show slight change when the thin film was annealed at 100 °C. The as-deposited IZO film had the lowest resistivity compared to the annealed IZO films. However there was an increase in resistivity by an order of magnitude from $3.3 \times 10^{-4}\,\Omega\,cm^2$ (as-deposited IZO films) to $2.9 \times 10^{-3}\,\Omega\,cm^2$, and reduction of carrier concentration from $5.8 \times 10^{20}\,cm^{-3}$ to $6.6 \times 10^{19}\,cm^{-3}$ as the annealing temperature was raised to 300 °C. The increase in resistivity can be attributed to the decrease of carrier concentration. In amorphous IZO films, intrinsic oxygen vacancies or interstitial Zn^{2+} ions act as dominant donors [11,13]. The results suggest that oxygen vacancies or interstitial Zn^{2+} ions could have annihilated due to oxygen incorporation during the annealing process leading to decrease in the carrier concentration of amorphous IZO films. The observation indicates the dependence of electrical conductivity of oxide materials on oxygen vacancies or interstitial Zn^{2+} ions and is in agreement with previous report [11,14]. The Hall mobility of the annealed IZO thin films did not change as noticeably as the carrier concentration and the resistivity did with annealing temperature. The Hall mobility showed a slight increase with the annealing temperature up to 200 °C and a subsequent decrease at 300 °C. The mobility in highly degenerated TCOs is affected by scattering centers such as ionized and neutral impurities, grain boundaries, lattice vibrations and dislocations. Among the above scattering centers, the ionized impurity scattering is the dominant scattering mechanism in amorphous IZO or ITO films and is closely related to the carrier concentration [11,15,16]. At higher carrier

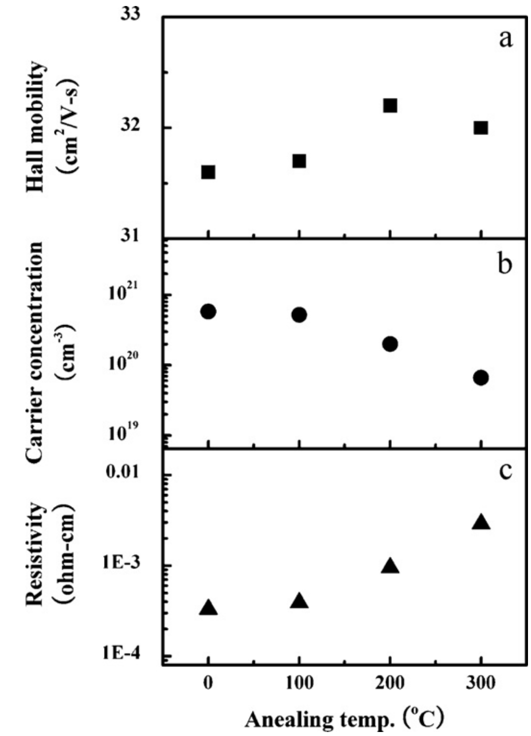

Fig. 2. (a) Hall mobility, (b) carrier concentration, (c) resistivity of the IZO films at different annealing temperature.

concentration ($>2.0 \times 10^{20}\,cm^{-3}$ in this result) the decrease of the Hall mobility with increasing the carrier concentration is attributed to the limitation imposed by ionized impurities scattering to the electron transport [16]. Ionized impurities originate from the oxygen vacancies in IZO. The oxygen vacancies are filled by oxygen during annealing in presence of oxygen resulting in the influence on mobility. In the present case the charge carriers in the IZO films might be affected by other scattering mechanism and exhibited smaller mobility than those previously reported by Ito et al. [11].

In Fig. 3 the optical transmittance of the IZO films in the wavelength range of 300–800 nm is displayed. The transmittance of the bare glass substrate was also measured for comparison and had a transmittance of 90%. The transmittance of the film annealed at 100 °C exhibited a similar trend to electrical properties, i.e. it did not show a noticeable change compared to the as-deposited film. The transmittance of the IZO films varied depending on the annealing temperature and the average transmittance decreased from 83.1%

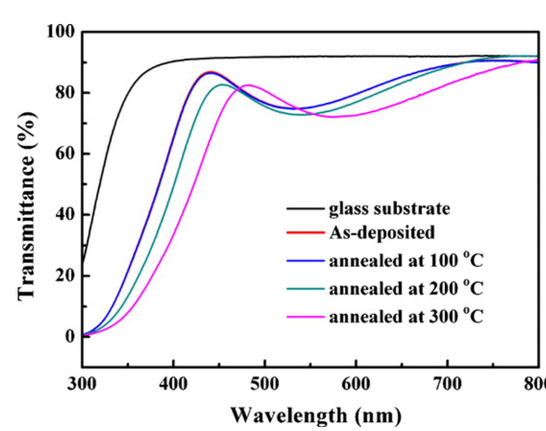

Fig. 3. Transmittance spectra of the as-grown IZO film and the films annealed at 100, 200 and 300 °C.

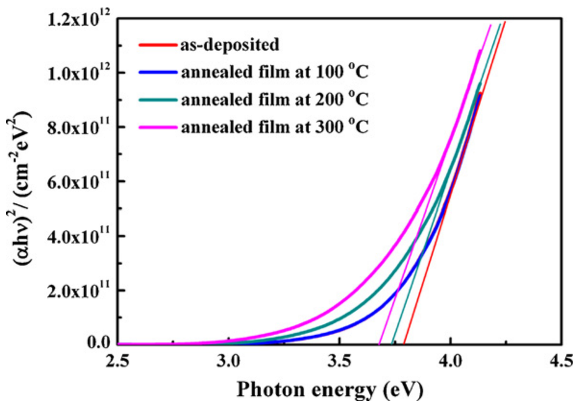

Fig. 4. $(\alpha h\upsilon)^2$ as a function of photon energies for the IZO films prepared under different conditions.

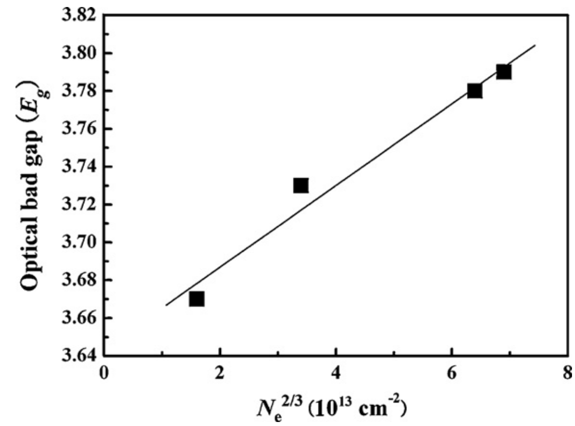

Fig. 5. Optical band-gap shift as a function of carrier concentration.

(as-deposited IZO film) to 76.7% (IZO film annealed at 300 °C) with the increase of the annealing temperature. It is further noted that the transmission edge progressively shifted toward lower energy with annealing temperature. The absorption coefficient (α) for a direct band-gap semiconductor can be evaluated using the following equation [17]:

$$\alpha = \ln \frac{(1/T)}{d}$$

where T is the transmittance and d is the film thickness. The optical band-gap is related to the absorption coefficient (α) and photon energy ($h\upsilon$) and can be calculated using the following relation [18]:

$$(\alpha h\upsilon)^2 = A(h\upsilon - E_{og})$$

where A is a constant and E_{og} is the optical band-gap of the material. Therefore the values of E_{og} can be determined by plotting $(\alpha h\upsilon)^2$ vs. photon energy and then extrapolating the linear regions of the plots to zero absorption. Fig. 4 shows the variation of $(\alpha h\upsilon)^2$ as a function of photon energy. The measured optical band-gap of the as-deposited film and the film annealed at 100 °C was observed to be nearly identical to each other. The optical band-gap was shifted toward the lower energy from 3.79 eV to 3.67 eV as the annealing temperature rose to 300 °C. In the case of degenerated semiconductors such as ITO, IZO and ZnO the optical band-gap is influenced by the change in carrier concentration and can be explained by either Burstein-Moss shift or band-gap narrowing effect. The widening (BM shift) of the optical band-gap occurs because lower states in the conduction band are blocked by the band filling for higher carrier concentration. The band-gap narrowing is known to be associated with various many-body interactions between the carriers in the conduction band and valence band called band-gap renormalization [9,21]. This operates simultaneously with the BM band-gap widening effect and reduces the magnitude of the optical band-gap. The many-body interactions are considered for high carrier densities i.e., $>10^{19}$ cm^{-3} [9,19,20]. In the present study, the carrier concentrations for all the IZO films are greater than 10^{19} cm^{-3} and therefore the optical band-gap shift as represented in Fig. 4 could result from the BM effect as well as band-gap renormalization. The relation between BM shift ΔE_g and the effective mass m^* is given as:

$$\Delta E_g = \frac{h^2(K_F)^2}{(8\pi 2m^*)},$$

where $K_F = (3\pi N_e)^{1/3}$ is the Fermi wave number, m^* is the effective mass, and N_e is the carrier concentration [21]. Since the IZO films are degenerated and have a large effective mass around $0.3m_0$ (m_0 being the effective mass of the free electron) [10], the optical band-gap shift is expected to be influenced more by the renormalization effect than the BM band-gap widening. However, in this case, even though IZO has a large effective mass of around $0.3m_0$, the shift of the optical band-gap was proportional to $N_e{}^{2/3}$ as shown in Fig. 5 as if only the BM band-gap widening effect was prevalent and that the renormalization did not play significant role in band-gap shifting. Though exact cause of such uncommon effect is not clear, this phenomenon could occur due to the overcompensation of band-gap narrowing effect by the BM widening effect which may happen for high carrier concentration [20].

4. Conclusion

Amorphous IZO films were deposited on glass substrates by radio frequency magnetron sputtering using the oxide ceramic In_2O_3–ZnO target. The changes in optical, structural, and electrical properties of the IZO films were investigated with the annealing temperature. The IZO films maintained the amorphous structure even after annealing at 300 °C. With the increase of the annealing temperature the resistivity decreased from $3.3 \times 10^{-4}\ \Omega\,cm^2$ (as-deposited IZO films) to $2.9 \times 10^{-3}\ \Omega\,cm^2$ and the optical band-gap shifted toward lower energy from 3.79 eV to 3.67 eV. Although all the IZO films were the degenerated semiconductors which had the high carrier concentration over 10^{19} cm^{-3} and large effective mass, the optical band-gap shift behaved as if only the BM band-gap widening effect is prevalent.

Acknowledgment

This work was supported by the National Research Foundation of Korea (NRF) funded by the Korea government (MEST) (2010-0019626, 2010-0026614, R01-2007-000-11177-0).

References

[1] H.–C. Cheng, C.–Y. Tsay, J. Alloys Compd. 507 (2010) L1.
[2] Y.L. Li, D.Y. Lee, S.R. Min, H.N. Cho, J.S. Kim, C.W. Chung, Jpn. J. Appl. Phys. 47 (2010) 6896.
[3] D.C. Paine, B. Yaglioglu, Z. Beiley, S.H. Lee, Thin Solid Films 516 (2008) 5894.
[4] K. Ramamoorthy, K. Kumar, R. Chandramohan, K. Sankaranarayanan, Mater. Sci. Eng. B 126 (2006) 1.
[5] H.–K. Kim, K.–S. Lee, J.H. Kwon, Appl. Phys. Lett. 88 (2006) 012103.
[6] Y. Yan, S.J. Pennycook, J. Dai, R.P.H. Chang, A. Wang, T.J. Marks, Appl. Phys. Lett. 73 (1998) 2585.
[7] T. Sasabayashi, N. Ito, M. Kon, P.K. Song, K. Ustumi, A. Kajio, Y. Shigesato, Thin Solid Films 445 (2003) 219.
[8] E. Burstein, Phys. Rev. 93 (1954) 632.
[9] A. Jain, P. Sagar, R.M. Mehra, Solid State Electron. 50 (2006) 1420.
[10] C. Marcel, N. Naghavi, G. Couturier, J. Salardenne, J.M. Tarascon, J. Appl. Phys. 91 (2002) 4291.

[11] N. Ito, Y. Sato, P.K. Song, A. Kaijio, K. Inoue, Y. Shigesato, Thin Solid Films 496 (2006) 99.
[12] M. Kamei, H. Akao, P.K. Song, I. Yasui, Y. Shigesato, Korean Ceram. Soc. 6 (2) (2000) 107.
[13] H.C. Pan, M.H. Shiao, C.Y. Su, C.N. Hsiao, J. Vac. Sci. Technol. A 23 (2005) 1187.
[14] D.Y. Ku, I.H. Kim, I. Lee, K.S. Lee, T.S. Lee, J.H. Jeong, B. Cheong, Y.J. Baik, W.M. Kim, Thin Solid Films 515 (2006) 1364.
[15] H. Han, J.W. Mayer, T.L. Alford, J. Appl. Phys. 100 (2006) 083715.
[16] A.J. Leenheer, J.D. Perkins, M.A. van Hest, J.J. Berry, R.P. O'Hayre, D.S. Ginley, Phys. Rev. B 77 (2008) 115215.
[17] V.R. Shinde, T.P. Gujar, C.D. Lokhande, R.S. Mane, S.H. Han, Mater. Chem. Phys. 96 (2006) 326.
[18] K. Zhang, F. Zhu, C.H.A. Huan, Thin Solid Films 376 (2000) 255.
[19] A.P. Roth, J.B. Webb, D.F. Williams, Phys. Rev. B 25 (1982) 7836.
[20] J.A. Sans, J.F. Sanchez-Royo, A. Segura, G. Tobias, E. Canadell, Phys. Rev. B 79 (2009) 195105.
[21] B. Kumar, H. Gong, R. Akkipeddi, J. Appl. Phys. 97 (2005) 063706.